

Conditions for jet break-out in neutron stars' mergers

Maxim Lyutikov

Department of Physics and Astronomy, Purdue University, 525 Northwestern Avenue, West Lafayette, IN 47907-2036

ABSTRACT

We consider conditions for jet break-out through ejecta following mergers of neutron stars and provide simple relations for the break out conditions. We demonstrate that: (i) break-out requires that the isotropic-equivalent jet energy E_j exceeds the ejecta energy E_{ej} by $E_j \geq E_{ej}/\beta_0$, where $\beta_0 = V_{ej}/c$, V_{ej} is the maximum velocity of the ejecta. If the central engine terminates before the break out, the shock approaches the edge of the ejecta slowly $\propto 1/t$; late break out occurs only if at the termination moment the head of the jet was relatively close to the edge. (ii) If there is a substantial delay between the ejecta's and the jet's launching, the requirement on the jet power increases. (iii) The forward shock driven by the jet is mildly strong, with Mach number $M \approx 5/4$ (increasing with time delay t_d); (iii) the delay time t_d between the ejecta and the jet's launching is important for $t_d > t_0 = (3/16)cM_{ej}V_{ej}/L_j = 1.01\text{sec}M_{ej,-2}L_{j,51}^{-1}(\beta_{ej}/0.3)$, where M_{ej} is ejecta mass, L_j is the jet luminosity (isotropic equivalent). For small delays, t_0 is also an estimate of the break-out time.

1. Introduction

During mergers of neutron stars (NSs, [Abbott et al. 2017](#); [Goldstein et al. 2017](#)) a dense wind is ejected (*e.g.*, [Lazzati et al. 2017](#); [Pozenenko et al. 2018](#); [Gottlieb et al. 2018](#)). Mass of the wind is $\sim \text{few } 10^{-2}M_\odot$ and the typical velocity is a fraction of the speed of light ([Metzger et al. 2010](#); [Barkov & Baushev 2011](#); [Kasliwal et al. 2017](#)).

At the same time the tidally stripped material forms an accretion disk that feeds the newly formed black hole (BH) with magnetic flux. After sufficient amount of the magnetic flux is accumulated, the Blandford-Znajek mechanism ([Blandford & Znajek 1977](#)) leads to jet launching, possibly with considerable delay ([Barkov & Pozenenko 2011](#); [Pozenenko et al. 2018](#)). As a result, the jet has to plow through the expanding ejecta. Depending on the parameters the jet may break out, or “fail” - just dissipate its energy within the ejecta ([Duffell et al. 2018](#)).

In this paper we consider the jet dynamics within an expanding ejecta and formulate criteria for the jet break out. There is number of numerical simulations of the problem (*e.g.*, [Aloy et al. 2005](#); [Duffell et al. 2018](#); [Gottlieb et al. 2018](#); [Hamidani et al. 2019](#)). Yet high computational costs involved in the simulations often preclude a detailed investigation of the parameter space, *e.g.*, the dependance of the jet dynamics on the properties of the ejecta, like maximal velocity (see, though a comment after Eq. (7)).

2. Constant driving

We assume that the ejecta expands homologously, with $v \propto r$, with constant proper density

$$\begin{aligned}\rho_{ej} &= \frac{3}{4\pi} \frac{M_{ej}}{(V_{ej}t)^3} \\ E_{ej} &= \frac{3}{10} M_{ej} V_{ej}^2, \\ v_r &= \frac{r}{t}, \quad r \leq V_{ej}t\end{aligned}\tag{1}$$

where M_{ej} and ρ_{ej} are total mass and density of the ejecta and V_{ej} is the maximal velocity; a more general scaling of ρ can also be used, $\rho \propto t^{-3}f(r/t)$, $v_r \propto (r/t)f(r/t)$, see [Chevalier \(1982\)](#) and [Appendix B](#). We assume that the maximal ejecta velocity is mildly relativistic at most, $\beta_{ej} = V_{ej}/c \leq 1$.

Consider first the case when a light, relativistic, constant power jet is launched into expanding ejecta by the central BH. To model the advancement of the jet's head we use the Kompaneets approximation ([Kompaneets 1960](#); [Bisnovatyi-Kogan & Silich 1995](#)). The Kompaneets approximation assume pressure balance between the jet and the ram pressure of the ejecta. It requires that the contact discontinuity is close to both the forwards shock in the ejecta and the termination shock in the jet. Under certain conditions it provides an excellent simple approximation (*e.g.*, [Marti et al. 1995](#); [Ramirez-Ruiz et al. 2002](#); [Matzner 2003](#); [Bromberg et al. 2011](#)).

We assume that the jet is launched with highly relativistic velocity, $v_j \approx c$. This requires jet to be sufficiently light. The composition of the jet is not important - only its' total power (or, in fact, thrust). On the other hand, we assume that the advancement of the jet's head is non-relativistic. This is justified since both the ejecta's velocity and the jets' head are expected to be mildly relativistic at most (for relativistic treatment see [Lyutikov 2012](#)).

The Kompaneets approximation aims to capture the overall dynamics of the shock, neglecting the details of the subsonic parts of the flow, *e.g.*, the formation of the cocoon (*e.g.*, [Komissarov & Falle 1998](#); [Morsony et al. 2007](#)). In fact, the Kompaneets approximation is momentum, not energy conserving. In what follows, we assume that the dynamics of the head of the jet is also self-similar, *e.g.*, no sideways expansion. This is justified if the properties of the jet at launching remain constant (*e.g.*, same opening angle).

In the Kompaneets approximation the shock radius $R(t)$ evolves according to (see [Appendix A](#))

$$\frac{L_j}{4\pi R^2 c} = \rho_{ej}(\dot{R} - R/t)^2 \quad (2)$$

Eq. (2) expresses a balance between the pressure of the relativistic jet and the ram pressure of the expanding ejecta. It is a generalization of the often-used momentum balance equation (eg [Begelman & Cioffi 1989](#), their Eq. (1)), to expanding and time-dependent external medium (see also [Bromberg et al. 2011](#); [Matzner 2003](#)). Relation (2) supersedes (in the relevant non-relativistic regimes) the related instantaneous approximation for velocity used in other works (*e.g.*, [Matsumoto & Kimura 2018](#); [Salafia et al. 2019](#); [Hamidani et al. 2019](#); [Gill et al. 2019](#)).

If the jet is launched with a delay t_d , the solution is

$$R = t \left(t^{1/2} - t_d^{1/2} \right)^{1/2} \frac{2L_j^{1/4} V_{ej}^{3/4}}{3^{1/4} c^{1/4} M_{ej}^{1/4}}, t \geq t_d \quad (3)$$

L_j is the isotropic equivalent jet power, t_d is delay time between the onset of the ejecta and switching on jet.

In Eq. (3) time $t = 0$ corresponds to the initial explosion. Shifting time to the moment the jet is initiated, we find the evolution equation for the expansion of the jet-driven bubble

$$R = (t + t_d) \left((t + t_d)^{1/2} - t_d^{1/2} \right)^{1/2} \frac{2L_j^{1/4} V_{ej}^{3/4}}{3^{1/4} c^{1/4} M_{ej}^{1/4}}, t \geq 0 \quad (4)$$

For very small delays $t_d \rightarrow 0$ Eq. (4) simplifies

$$R = \frac{2}{3^{1/4}} \frac{L_j^{1/4} V_{ej}^{3/4}}{c^{1/4} M_{ej}^{1/4}} t^{5/4} \quad (5)$$

In this case the break out at $R = V_{ej}t$ occurs at time and distance

$$t_0 = \frac{3}{16} \frac{cM_{ej}V_{ej}}{L_j} = 1.01 \text{sec} M_{ej,-2} L_{51}^{-1} \left(\frac{\beta_{ej}}{0.3} \right) \quad (6)$$

$$R_0 = V_{ej}t_0 = \frac{3}{16} \frac{cM_{ej}V_{ej}^2}{L_j} = 9 \times 10^9 \text{cm} M_{ej,-2} L_{51}^{-1} \left(\frac{\beta_{ej}}{0.3} \right)^2 \quad (7)$$

Time t_0 is a typical time of the jet-ejecta interaction.

Relations (6-7) provide clear simple estimates for the break-out moment and radius. For example, relation (6) explains the result of Gill et al. (2019), their Fig. 5, which shows longer break-out times in the faster-expanding ejecta.

For finite delay times t_d the edge of the ejecta is at $R = V_{ej}(t + t_d) = \beta_0 c(t + t_d)$ (time t is counted from the jet's initiation, not from the initial explosion). Thus, the delay between the expulsion of the ejecta and turning-on of the jet is important for $t_d > t_0$.

At a given moment the shock velocity is

$$V_s = \partial_t R = \frac{\beta_0^{3/4}}{2 \times 3^{1/4}} \left(\frac{5\sqrt{t+t_d} - 4\sqrt{t_d}}{\sqrt{\sqrt{t+t_d} - \sqrt{t_d}}} \right) \left(\frac{\sqrt{c} L_j^{1/4}}{M_{ej}^{1/4}} \right) \quad (8)$$

At the location of the shock the upstream velocity is

$$v_1 = \frac{R}{t+t_d} = \frac{2\beta_0^{3/4}}{3^{1/4}} \sqrt{\sqrt{t+t_d} - \sqrt{t_d}} \frac{\sqrt{c} L_j^{1/4}}{M_{ej}^{1/4}} \quad (9)$$

So that the Mach number is

$$M = \frac{V_s}{v_1} = \frac{5\sqrt{t+t_d} - 4\sqrt{t_d}}{4(\sqrt{t+t_d} - \sqrt{t_d})} \rightarrow \frac{5}{4} \quad (10)$$

where the last relation assumes $t_d = 0$. For longer delays the Mach number is larger. Thus, the forward shock is mild regardless of the jet power. (Stronger jets quickly drive the shock further out, where the velocity of the ejecta is larger.)

Let's renormalize time by

$$\begin{aligned} t_0 &= \frac{3}{16} \frac{cM_{ej}\beta_0 c}{L_j} \\ \hat{t} &= \frac{t}{t_0} \end{aligned} \quad (11)$$

and the radius of the jet-blown cavity by the overall radius of the ejecta:

$$\hat{R} = \frac{R}{\beta_0 c(t+t_d)} < 1 \quad (12)$$

Value of \hat{R} corresponds to the relative value of the jet-blown bubble with respect to the overall radius of the ejecta.

In dimensionless units

$$\hat{R} = \sqrt{\sqrt{\hat{t} + \hat{t}_d} - \sqrt{\hat{t}_d}} \approx \begin{cases} \hat{t}^{1/4}, & \hat{t}_d \rightarrow 0 \\ \frac{1}{\sqrt{2}} \frac{\hat{t}^{1/2}}{\hat{t}_d^{1/4}}, & \hat{t}_d \rightarrow \infty \end{cases}, \quad (13)$$

see Fig. 1.

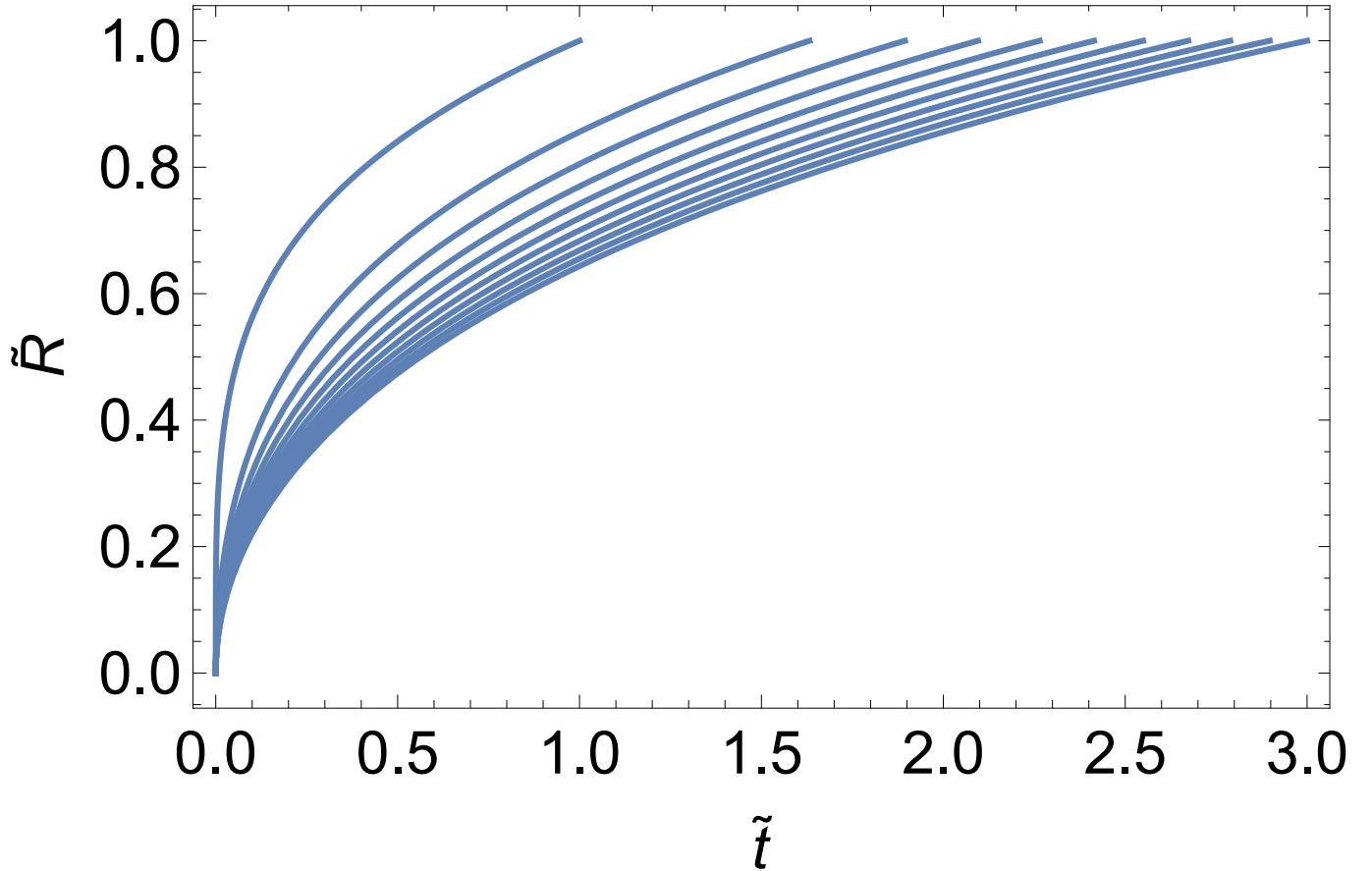


Fig. 1.— Radius of the jet-driven bubble as a function of time for constant jet power, normalized to the total radius of the ejecta. Different curves correspond to different delay times, $\hat{t}_d = 0, .1, \dots, 1$ (top to bottom). Moments when $\hat{R} = 1$ (occurring at $\hat{t}_{br} = 1 + 2\sqrt{\hat{t}_d}$) correspond to jet break-out. Corresponding physical distance is given by Eq. (14).

The break out is at $\hat{R} = 1$; it occurs at time \hat{t}_{br} and physical distance R_{br}

$$\begin{aligned} \hat{t}_{br} &= 1 + 2\sqrt{\hat{t}_d} \\ \frac{R_{br}}{R_0} &= 1 + 2\sqrt{\frac{\hat{t}_d}{t_0}} \end{aligned} \quad (14)$$

At the break out the energy deposited by the jet satisfies

$$E_j = L_j t_{br} = \frac{5(1 + 2\sqrt{\hat{t}_d/t_0})}{8\beta_0} E_{ej} \quad (15)$$

(since we are in a regime $\beta_0 \ll 1$ we neglect the difference between the emitted and absorbed power). Thus, in order to break out during jet activity even with small delay $\hat{t}_d \ll 1$, the required total jet energy is fairly large, $E_j \approx E_{ej}/\beta_0$.

3. Late break-outs

Suppose next that the central engine stops producing a jet before the head of the jet breaks out from the ejecta. At this moment the jet has swept some mass and moment from the ejecta, as well as deposited momentum in the shocked ejecta shell. After the switching-off of the engine the shocked ejecta shell starts to relax as the reverse shock in the jet propagates back to the origin. This takes relatively long time, so for the times scales of interest, few seconds, the system never reaches fully relaxed Sedov stage.

Previously Lyutikov (2011) discussed evolution of a non-spherical shock in a steep density gradient of expanding envelope of the exploding star (in application to long GRBs), taking into account the sideways expansion of the jet-driven bubble. The approach of Lyutikov (2011) follows the original Kompaneets pressure-equilibrating prescription (Kompaneets 1960). Irwin et al. (2019) followed this procedure in details.

It is not clear if pressure-equilibrating assumption is applicable to the jet propagating in short GRBs. Typically, pressure equilibration takes few dynamical times. In case of long GRBs, the velocity of the heads is expected to be highly sub-relativistic, allowing for pressure equilibration. In the present case both the expansion velocity and the sound speed are mildly relativistic, so pressure equilibrium within the cocoon is likely not reached fast enough.

A related approximation that can be used is the snowplow: we assume that the shell propagates in momentum-conserving (snowplow) state. After the engine stops, the momentum of the swept up shell with mass M_s changes due to the swept-up momentum P_s :

$$\begin{aligned}\partial_t(M_s\partial_t R) &= \partial_t P_s \\ M_s &= 4\pi \int_0^R \rho_{ej} r^2 dr = M_{ej} \frac{R^3}{(c\beta_0(t+t_d))^3} \\ P_s &= 4\pi \int_0^R \rho_{ej} \frac{r}{t+t_d} r^2 dr = \frac{3}{4} \frac{M_{ej} R^4}{(t+t_d)^4 (c\beta_0)^3} \\ \rho_{ej}(t) &= \frac{3}{4\pi} \frac{M_{ej}}{(c\beta_0(t+t_d))^3}\end{aligned}\tag{16}$$

Eq. (16) becomes

$$R((t_d+t)^2 \partial_t^2 R + 3R) + 3(t_d+t)^2 (\partial_t R)^2 - 6R(t_d+t) \partial_t R = 0\tag{17}$$

which has a solution

$$R_{after} = (t+t_d)^{3/4} (C_1 t + C_2)^{1/4}\tag{18}$$

where coefficient C_1 and C_2 are integration constants. Converting to dimensionless units

$$\hat{R}_{after} = \frac{(\hat{C}_1 \hat{t} + \hat{C}_2)^{1/4}}{(\hat{t} + \hat{t}_d)^{1/4}}\tag{19}$$

Coefficients \hat{C}_1 and \hat{C}_2 in Eq. (19) can be derived from the condition that the radii immediately before the switch-off, Eq. (13) and after, Eq (19), match,

$$\begin{aligned}\hat{C}_1 &= 3\hat{t}_d + 2\hat{t}_{off} - \sqrt{\hat{t}_d(\hat{t}_d + \hat{t}_{off})} \\ \hat{C}_2 &= 2\hat{t}_d^2 - \hat{t}_{off}^2 + (\hat{t}_{off} - 2\hat{t}_d) \sqrt{\hat{t}_d(\hat{t}_d + \hat{t}_{off})}\end{aligned}\tag{20}$$

Asymptotically, $\hat{t} \rightarrow \infty$, the shell is just advected with the flow,

$$\hat{R}_{after} \approx f_1(\hat{t}_d, \hat{t}_{off}) + f_2(\hat{t}_d, \hat{t}_{off}) \frac{1}{\hat{t}}\tag{21}$$

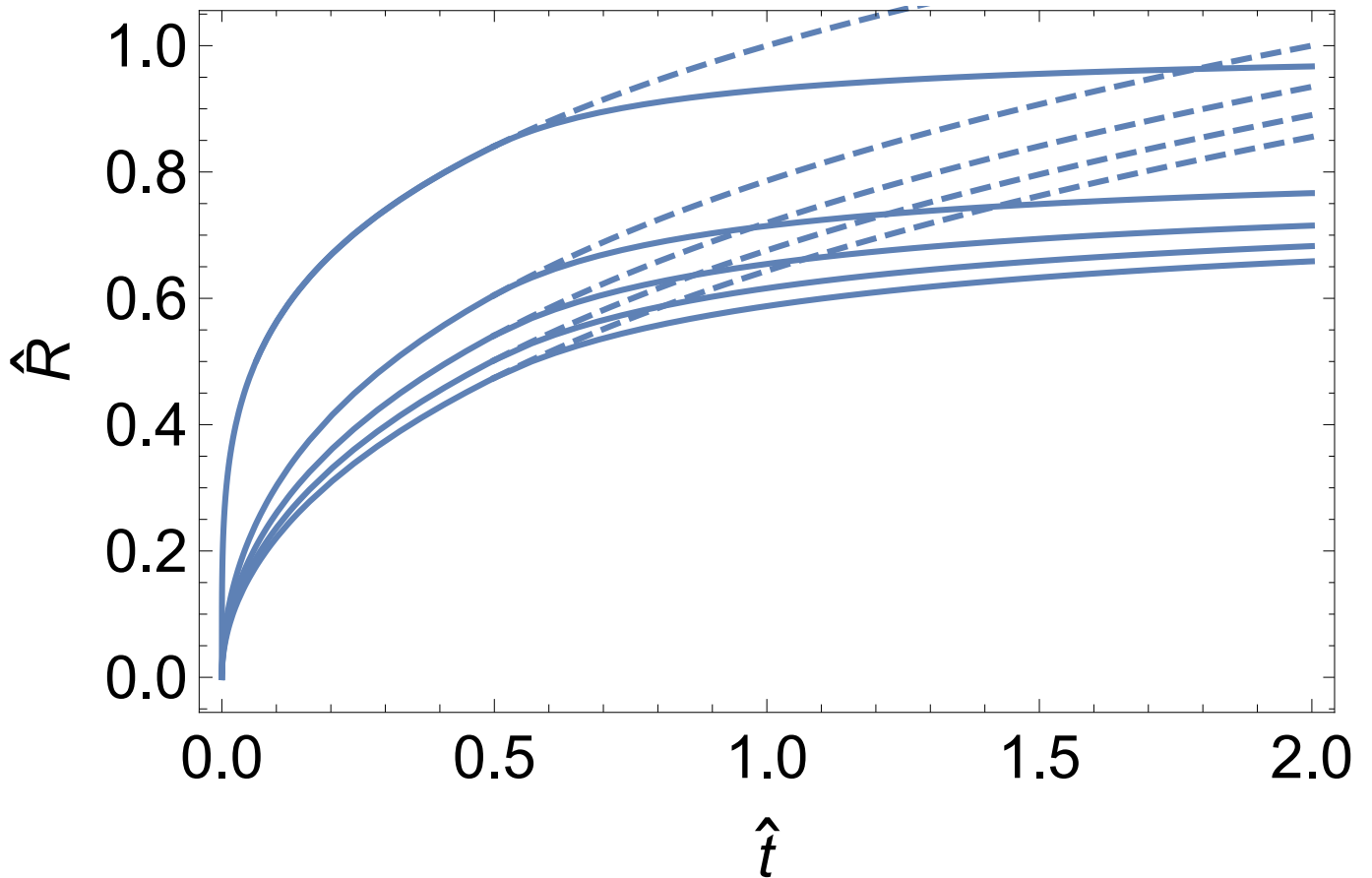


Fig. 2.— Relative radius of the jet-driven bubble as a function of time. At $\hat{t}_{off} = 1/2$ the jet is turned off. Different curves correspond to $\hat{t}_d = 0, 0.25, 0.5, 0.75, 1$ (top to bottom). After the jet is turned off the shock quickly reaches the coasting phase. Dashed lines for $\hat{t} \geq \hat{t}_{off} = 1/2$ correspond to the case without jet termination

where f_1 and f_2 are some function of \hat{t}_d and \hat{t}_{off} . Thus, if the jet did not break out during the active phase, after the termination of the injection the head of the jet advances (with respect to the ejecta’s flow) very slowly $\propto \hat{t}^{-1}$, see Fig. 2. Particular values of coefficients (20) are not relevant, and highly dependent on the assumed analytical approximations.

Thus, we find that the shock approaches the edge of the ejecta very slowly as a decreasing power-law, $\Delta\hat{R} \propto -1/t$. As a result, we conclude that any analytical approximation to the late break out is likely to depend on the subtle assumed details. Numerical models are more reliable in this case (Aloy et al. 2005; Duffell et al. 2018; Gottlieb et al. 2018; Hamidani et al. 2019).

4. Conclusion

In this paper we considered conditions for the break-out of the BH-launched jet from the envelope of the ejecta material in neutron star mergers. We provide clear simple estimates (14) for the jet break times and conditions. Simplicity or relations (14) is quite remarkable if compared with previous similar previous approaches. The direct break

out condition (15) requires that the total energy in jet should exceed the energy in the ejecta by at least a factor $1/\beta_0 \geq 1$. If there is a substantial delay between the ejecta’s launch and the formation of the jet, the requirement on the jet’s total energy mildly increases. Late break outs occur only if the head of the jet relatively close to the edge of the ejecta at the moment when the engine shuts off.

Acknowledgments

This work had been supported by NASA grant 80NSSC17K0757 and NSF grants 10001562 and 10001521. I would like to thank Maxim Barkov and Paul Duffell for discussions and comments on the manuscript.

REFERENCES

- Abbott, B. P., Abbott, R., Abbott, T. D., Acernese, F., Ackley, K., Adams, C., Adams, T., Addesso, P., Adhikari, R. X., Adya, V. B., & et al. 2017, *ApJ*, 848, L13
- Aloy, M. A., Janka, H. T., & Müller, E. 2005, *A&A*, 436, 273
- Barkov, M. V., & Baushev, A. N. 2011, *New A*, 16, 46
- Barkov, M. V., & Pozanenko, A. S. 2011, *MNRAS*, 417, 2161
- Begelman, M. C., & Cioffi, D. F. 1989, *ApJ*, 345, L21
- Bisnovaty-Kogan, G. S., & Silich, S. A. 1995, *Reviews of Modern Physics*, 67, 661
- Blandford, R. D., & Znajek, R. L. 1977, *MNRAS*, 179, 433
- Bromberg, O., Nakar, E., Piran, T., & Sari, R. 2011, *ApJ*, 740, 100
- Chevalier, R. A. 1982, *ApJ*, 258, 790
- Duffell, P. C., Quataert, E., Kasen, D., & Klion, H. 2018, *ApJ*, 866, 3
- Gill, R., Nathanail, A., & Rezzolla, L. 2019, *ApJ*, 876, 139
- Goldstein, A., Veres, P., Burns, E., Briggs, M. S., Hamburg, R., Kocevski, D., Wilson-Hodge, C. A., Preece, R. D., Poolakkil, S., Roberts, O. J., Hui, C. M., Connaughton, V., Racusin, J., von Kienlin, A., Dal Canton, T., Christensen, N., Littenberg, T., Siellez, K., Blackburn, L., Broida, J., Bissaldi, E., Cleveland, W. H., Gibby, M. H., Giles, M. M., Kippen, R. M., McBreen, S., McEnery, J., Meegan, C. A., Paciasas, W. S., & Stanbro, M. 2017, *ApJ*, 848, L14
- Gottlieb, O., Nakar, E., Piran, T., & Hotokezaka, K. 2018, *MNRAS*, 479, 588
- Hamidani, H., Kiuchi, K., & Ioka, K. 2019, arXiv e-prints, arXiv:1909.05867
- Irwin, C. M., Nakar, E., & Piran, T. 2019, *MNRAS*, 489, 2844
- Kasliwal, M. M., Nakar, E., Singer, L. P., Kaplan, D. L., Cook, D. O., Van Sistine, A., Lau, R. M., Fremling, C., Gottlieb, O., Jencson, J. E., Adams, S. M., Feindt, U., Hotokezaka, K., Ghosh, S., Perley, D. A., Yu, P. C., Piran, T., Allison, J. R., Anupama, G. C., Balasubramanian, A., Bannister, K. W., Bally, J., Barnes, J., Barway, S., Bellm,

E., Bhalerao, V., Bhattacharya, D., Blagorodnova, N., Bloom, J. S., Brady, P. R., Cannella, C., Chatterjee, D., Cenko, S. B., Cobb, B. E., Copperwheat, C., Corsi, A., De, K., Dobie, D., Emery, S. W. K., Evans, P. A., Fox, O. D., Frail, D. A., Frohmaier, C., Goobar, A., Hallinan, G., Harrison, F., Helou, G., Hinderer, T., Ho, A. Y. Q., Horesh, A., Ip, W. H., Itoh, R., Kasen, D., Kim, H., Kuin, N. P. M., Kupfer, T., Lynch, C., Madsen, K., Mazzali, P. A., Miller, A. A., Mooley, K., Murphy, T., Ngeow, C. C., Nichols, D., Nissanke, S., Nugent, P., Ofek, E. O., Qi, H., Quimby, R. M., Rosswog, S., Rusu, F., Sadler, E. M., Schmidt, P., Sollerman, J., Steele, I., Williamson, A. R., Xu, Y., Yan, L., Yatsu, Y., Zhang, C., & Zhao, W. 2017, *Science*, 358, 1559

Komissarov, S. S., & Falle, S. A. E. G. 1998, *MNRAS*, 297, 1087

Kompaneets, A. S. 1960, *Soviet Physics Doklady*, 5, 46

Lazzati, D., López-Cámara, D., Cantiello, M., Morsony, B. J., Perna, R., & Workman, J. C. 2017, *ApJ*, 848, L6

Lyutikov, M. 2011, *MNRAS*, 411, 2054

—. 2012, *MNRAS*, 421, 522

Marti, J. M. A., Muller, E., Font, J. A., & Ibanez, J. M. 1995, *ApJ*, 448, L105

Matsumoto, T., & Kimura, S. S. 2018, *ApJ*, 866, L16

Matzner, C. D. 2003, *MNRAS*, 345, 575

Metzger, B. D., Martínez-Pinedo, G., Darbha, S., Quataert, E., Arcones, A., Kasen, D., Thomas, R., Nugent, P., Panov, I. V., & Zinner, N. T. 2010, *MNRAS*, 406, 2650

Morsony, B. J., Lazzati, D., & Begelman, M. C. 2007, *ApJ*, 665, 569

Pozanenko, A. S., Barkov, M. V., Minaev, P. Y., Volnova, A. A., Mazaeva, E. D., Moskvitin, A. S., Krugov, M. A., Samodurov, V. A., Loznikov, V. M., & Lyutikov, M. 2018, *ApJ*, 852, L30

Ramirez-Ruiz, E., Celotti, A., & Rees, M. J. 2002, *MNRAS*, 337, 1349

Salafia, O. S., Barbieri, C., Ascenzi, S., & Toffano, M. 2019, arXiv e-prints, arXiv:1907.07599

A. Relativistic Kompaneets equation

Consider interaction of two cold flows with rest frame enthalpies $w_{1,2}$ each moving with Lorentz factor $\Gamma_{1,2}$. In the Kompaneets approximation (in a sense that only momentum conservation is used), the internal dynamics in the shock regions is neglected. Then in the rest frame of the contact discontinuity

$$u_1^2 w_1 = u_2^2 w_2 \tag{A1}$$

where $u_{1,2}$ are momenta of fluids.

Let v_w be the wind velocity in the lab frame, v_{ex} the upstream velocity in the lab frame, and v_s is the shock velocity. Since $w_{1,2}$ are Lorentz invariant quantities, $w_1 = w_w$, $w_2 = w_{ex}$. Using relativistic transformations one finds (Matzner 2003)

$$\begin{aligned} v_s &= \frac{v_{ex}/\sqrt{\mathcal{L}} + v_w}{1 + 1/\sqrt{\mathcal{L}}} \\ \mathcal{L} &= \frac{\Gamma_w^2 w_w}{\Gamma_{ex} w_{ex}} \end{aligned} \quad (\text{A2})$$

Using expression for the luminosity of a spherical wind

$$L_w = 4\pi R^2 \Gamma_w^2 w_w v_w \quad (\text{A3})$$

one finds

$$\frac{L_w}{4\pi R^2 v_w} = w_{ex} \Gamma_{ex}^2 \frac{(v_s - v_{ex})^2}{(v_w - v_s)^2} \quad (\text{A4})$$

For $v_w \approx c$, $w_{ex} = \rho_{ex} c^2$ and $v_s \ll v_w$, Eq. (A4) reduces to (2) for $v_s = \partial_t R$ and $v_{ex} = R/t$.

B. More general density profiles

For ejecta's density

$$\rho = \frac{3-n}{4\pi} \frac{M_{ej}}{(V_{ej}t)^3} \left(\frac{r}{V_{ej}t} \right)^{-n} \quad (\text{B1})$$

the jet's head radius evolves according to (see also Lyutikov 2011)

$$\begin{aligned} R &= (t + t_d) \left((t + t_d)^{1/2} - t_d^{1/2} \right)^{2/(4-n)} \left(\sqrt{\frac{L_j}{cM_{ej}}} \frac{(4-n)}{\sqrt{3-n}} V_0^{(3-n)/2} \right)^{2/(4-n)} \\ R &= t^{(5-n)/(4-n)} \left(\sqrt{\frac{L_j}{cM_{ej}}} \frac{(4-n)}{\sqrt{3-n}} V_0^{(3-n)/2} \right)^{2/(4-n)}, \text{ for } t_d = 0 \end{aligned} \quad (\text{B2})$$

The corresponding relative distance to the break out is $\hat{R} \propto \hat{t}^{1/(4-n)}$. For no delay, the breakout is at

$$t'_0 = \frac{(3-n)}{(4-n)^2} \frac{cM_{ej}V_{ej}}{L_j} \quad (\text{B3})$$

If time is normalize to (B3) and distance to $V_0 t'_0$, the break out occurs at (14) regardless of the index n .